Selective Spectral Coding for TPS selection in Thermal Error Analysis

[1] S KARTHIK, [2] MOYYA SUNDEEP

M.Tech , Thermal Engineering ,

MLR Institute of Technology,

Dundigal, Hyderabad

Assistant Professor, Dept of Mechanical,

MLR Institute of Technology,

Dundigal, Hyderabad

Abstract- Machine tools are crucial in the manufacturing industry for producing products with high quality and accuracy while reducing expenses and production time. One significant problem affecting precision machining accuracy is thermal inaccuracy. It is mostly produced due to thermal expansion and contraction in machine while it is operating, particularly thermal deformation, which considerably influences the end product's accurateness. Currently, thermal deformation is predicted using mathematical models, and real-time compensation is achieved by Computer Numerical Control (CNC) systems. Temperature Sensitive Points (TSP) must be identified in order to create precise thermal fault forecast models. Due to the nonlinear allocation of high temperature sources in machine equipment, the present approach employs simulations by means of the limited element means and cluster analysis to identify temperature locations that are closely associated with thermal errors. However, the dynamic adjustment of thermal properties leads to a numerical control error that damages the tool. To improve the controlling system's accuracy, a selective learning approach for temperature analysis is suggested.

Keyword: Thermal analysis, signal anomaly, selective coding, and numerical controlling.

I. Introduction

A system's thermal deformation process has to be tracked and managed for optimal performance, durability, safety, and economy across a range of applications. Due mostly to concerted efforts in experimental research and numerical modelling, our understanding of the principles of thermal deformation has greatly improved over time. Because of the unique contributions that various disciplines of study have made, the body of knowledge has expanded. The advancement of artificial intelligence and large information processing has made it impossible for conventional machine learning techniques to fulfil the increased accuracy requirements. Machine tool thermal error Modelling has advanced and gained new possibilities thanks to deep learning techniques. Deep learning techniques are separated into two groups in this section: those that use temperature information as input. According to reports, thermal errors report for over 75% of CNC machine tool's overall positioning error [1], however this varies from machine to machine. Higher accuracy is also needed on big machine tools due to the growing demand for huge, expensive components like engine blocks, aerofoils, impeller blades, etc. Because mistakes necessarily grow with machine size and axis count, the accurateness of machine tools typically lagged 3-axis machine tools. It is very vital to provide an effective Modelling solution for such devices. The impact of temperature variations on precision of machine tools has received consideration in recent past [2–5]. Heat sources within the machine tool's construction and dissimilarity in surrounding temperature are main causes of thermal fluctuations in the tool's structure. Drive motors, gear trains, and other components are examples of internal heat sources. Nonetheless, there are two types of heat sources that surround a machine tool [6]. Those that are within the machine and those those are outside of it. Every heat mean which are physically attached to machine tool frame are regarded as internal heat sources. They induce thermal reaction and deformations by directly conducting heat into the machine structure. Numerous papers have focused on comprehending the impact of each of these sources [7–8]. According to the study, one of the primary causes of heat production and the ensuing deformations is thought to be the spindle system and its bearings. The temperature produced by spindle process result in temperature deviations in machine components if error prevention techniques, such a cooling jacket, are not used. Thermal imaging is often used in this thesis to quickly evaluate the machine tool's interior heat sources. The actual cutting operation, which heats the tool, tool holder, clamping mechanism, and work piece, is another significant internal heat source. The machining process's friction Modelling has been the subject of much study [9], but the thermal characteristics of the process have not received enough attention [10]. Hot chips from the cutting operation might also indirectly heat up the table, another component. Cutting fluid (coolant) may be used to lessen this heat source. However, such a method must only be employed with careful caution since it might produce extra negative heat sources. The machine's surroundings, including nearby machines, the opening and shutting of machine entry, changes in the ambient temperature over daytime and night-time sequence, and seasonal variations in behaviour, are considered external heat sources. Because of the difficulty of the nearby working surroundings and the overall funds concern, maintaining a homogenous and stable machine thermal environment is not a simple task. The machine's electrical cabinet and lighting are two minor heat sources that have the potential to significantly alter the machine's structure. The interplay between these many heat sources produces a machine's complicated thermal behaviour. In relation to a work piece, and depending on where they come from, they may or may not be reliant on the axis position. Both temperature and axis locations affect position-dependent thermal errors [11]. The spindle's heat may cause some of them to alter rapidly, while the ambient temperature may cause others to change more slowly. Depending on the machine's shape, various thermal changes might unite, while other's might cancel-out. Thermal errors may result from the history of the machining process, heat sources associated with moving axes, and fluid flow, which varies depending on the operation the machine, is doing. The intricacy of the thermal error issue led to the creation of several methods and techniques to lessen its impact. By modifying via sophisticated manufacturing techniques, source isolation, thermal errors may be decreased. These procedures are best used during the machine tool's design phase. The machine tool frame and its assemblies may be designed to be insensitive to temperature fluctuations as feasible by considering their material and shape. This isn't always feasible, however, because of the expense and potential compromises on things like accessibility for the tool changer's part-loading site, overall footprint, etc. In order to accurately detect all naturally occurring events, the machine tool's numerical Modelling have to take in the common relations among heat sources [12]. FEA, or finite element analysis, is an extremely useful technique, particularly when designing a new machine. Accurate understanding of the impact of many parameters on thermal behaviour of machine tools is achieved via their application [13]. This makes it possible to choose how the machine's components, structure, and heat sources are arranged. Usually, optimization of size, capital, and operating expenses determines the ultimate design. Some design modifications that have greatly aided in lowering thermal errors are listed below:

• A key factor in the deformation behaviour is the machine's geometry [14]. Reduced distortions and temperature gradients are the results of a machine construction that is thermally symmetrically designed [15]. For instance, in order to ensure symmetrical design and balanced thermal behaviour, machine elements like rams and columns often have a square form. Using a simulation analysis, [16] suggested several design changes for a lathe model and conducted evaluation. The example shows how design changes may lower the prototype's thermal inaccuracy to about 15% of its initial value. Additionally, to lessen thermal deformation, a lightweight construction with slight walls advised (for lower heating capability) [17]. However, it is critical for machine tool developer to comprehend the actual implementation of the lightweight construction.

• Making use of materials such polymer concrete, fiber-reinforced polymers, and cast iron that have a higher detailed heating limit and a lower thermal extension parameter [18]. Cast iron is mainly used object in the machine tool industry because of its stability, ease of casting, and cost-effectiveness in machining. However, since polymer concrete may be utilized in industrial bases that need material features like strong heat stability, it has drawn more attention.

[19] Observed at how the affect of various aggregate compositions on thermal expansion was using ANSYS software. Their findings indicate that basalt, sand, and fly ash, in that order, have the lowest factor of thermal

expansion and the most suitable flexural power, making them the ideal composition of the region they studied. One major cause of positioning inaccuracy may be the ball screw shaft's thermal distortion. When a ball screw system operates normally, heat produced by the balls' frictional action on the thread causes the screw's temperature to rise significantly. Direct feedback may be obtained by eliminating the ball screw from the positioning loop using linear or laser scales. However, it may be expensive and technically challenging to fit such scales to many machinery [20]. Furthermore, practical scale placements may not be optimal from a thermal perspective, thus they cannot be regarded as a comprehensive solution to the issue. Applying pretension to the ball screw is another popular method for lessening the impact of ball screw expansion. There are many disadvantages to this method, including the possibility of vibration, and bearing malfunction issues [21]. With the developments in past, it is observed that machine tools need precise and accurate processing of thermal error detection. In processing accurate thermal error detection, selection of processing coefficients and compensation are primal requirements. To achieve a finer selection of thermal coefficients and process for compensation, this paper present a learning based approach for processing and feature analysis in thermal error detection. To present the outlined work this paper is presented in 5 sections. Where section 2 present the conventional method of thermal error detection. Section 3 outlines the method of TSP selection using selection process. Experimental result for the outlined work is presented in section 4 and section 5 presents the conclusion of the work.

II. Thermal error modelling and compensation

The main significant issue which affects the machine accurateness is thermal error developed by thermal deformation. The spindle is a primary heat input that causes thermal distortions out of all of them. When compared to other thermal error management and reduction techniques, analytical computation, numerical analysis, and experimental testing. There is a list and discussion of the many approaches used in testing, Modelling, and compensating. Furthermore, several methods for selecting thermal main points are shown as they are essential for testing, thermal error analysis, and also affect how well compensation works.

Numerous studies have been conducted for thermal error modelling, with the goal of choosing TSPs with high correlation and low co-linearity in reference to construct a thermal system with higher accurateness and resilience. The thermal error Modelling used is presented as below.

Assuming thermal error is represented by E and there are n temperature observing locations, given as Th_i,..., $Th_{i,n}$. For m times of information observations the data collected during the measurement and are indicated by,

$$Th_i = (th_{1,1,}, \dots., th_{1,n}) \quad (1)$$

$$Th_{i,m} = (th_{m,1,}, \dots., th_{m,n} \quad (2)$$

$$E = (e_{1,1,}, \dots., e_{1,n}) \quad (3)$$

a) Thermal Error Modeling Algorithms

Measurement information’s are applied to construct thermal error unit. The system input the TSPs, and it output thermal error. Two most popular algorithms are multiple regression and neural network. These two algorithms vary in their architecture and training strategies. The steepest descent method is a popular technique for training neural networks (NNs) by continually varying the connection weights between nodes. For space considerations, the NN will not be described in further depth since the regression technique is the primary focus of this study. The multiple regression approach has a polynomial model structure. The high degree of co-linearity in the model input for ordinary multiple regressions will raise the approximate inconsistency of the model data, creating the model unbalanced and prone to over fitting. When there is strong co-linearity input, ridge regression may greatly decrease variance by adding up a converging element to the loss function. The following is how the model is expressed:

$$E' = \gamma_0 + \gamma_1 Th_1 + \cdots \dots + \gamma_n Th_{ns} \quad (4)$$

Where ns represents number of TSPs, $E^{'}$ the thermal error, and Th_1–Th_{ns} are TSPs. The following equation may be used to estimate model elements γ by ridge regression given as,

$$\gamma = (K^T K + P_r I)^{-1} K^T E \quad (5)$$

where P_r is ridge value and I defines identity matrix. Prior work gave P_r values between 10 and 30.

b) Selection of TSP and Thermal Error Update

Temperature-sensitive points (TSPs) in machine tools are particular places where variations in temperature significantly affect thermal change and, therefore, the accuracy of the machine. For precise thermal error Modelling and improvement in machine operation, these considerations are essential. TSPs are carefully chosen measurement locations on the machine tool arrangement where changes in temperature significantly impact the total amount of thermal deformation.

• TSPs' function:

• Accurate Thermal Error Modelling: Thermal error models, which forecast how the machine will deform at various temperatures, are made using TSPs.
• Efficient Thermal Compensation: Machine tools may improve machining precision by compensating for thermal deformation by applying the thermal error model and monitoring temperatures at TSPs. Choosing TSPs: There are many ways to choose TSPs, such as:

Finding locations where temperature variations and thermal deformation have a strong association is known as correlation analysis.

• Finite Element Analysis (FEA): Identifying vulnerable regions and analyzing heat behaviour using FEA simulations.

• Statistical Techniques: To ascertain the connection between temperature and deformation, statistical techniques such as regression analysis are used. TSP importance: Choosing the right TSPs is essential for creating precise thermal error models and efficient compensation plans, both of which have a direct influence on the machine tool's accuracy.

c) TSP Selection Method

Different groups are created from the first temperature measurement locations. While various groups have low co-linearity, the same group has high co-linearity. One such approach is selective clustering. Using distance as the correlation coefficient between Si and Sj, create a selected similarity matrix S. Create an equivalent matrix from a similarity matrix. Selective similarity matrices may be subjected to the following multiple square selective operations:

$$S \times S = S^2 \quad (6)$$

$$S^2 \times S^2 = S^4 \quad (7)$$

$$S^{2n} \times S^{2n} = S^{2(n+1)} \quad (8)$$

The following is the square selection operation.

$$S \times S = [s_{i,j}{}^2] \quad (9)$$

$\boldsymbol{s_{i,j}}$ is a selected equivalent matrix if it equals $\boldsymbol{S^{2(n+1)}}$. Making the selective relationship transitive is the goal of changing the selected equivalent matrix.

L be the threshold, $F(Si, Sj) > L$ if Si and Sj belong to the same group. It is decided how many groups and TSPs there are. L_{TSP} has the highest correlation among all temperature measurement. The correlation coefficient is given by,

$$\partial_{Si,E} = \frac{\sum_{i=1}^{m}(s_i - s_i^{'})(e_i - e_i^{'})}{\sqrt{\sum_{i=1}^{m}(s_i - s_i^{'})\sum_{i=1}^{m}(e_i - e_i^{'})}} \quad (10)$$

where s_i and e stand for the information's respective averages, Si and E.

d) Stability of Selection of TSP

Greater association and low co-linearity are opposing states for TSPs. Specifically; the grouping method lowers the correlation and co-linearity of TSPs. Given that the co-linearity issue may be resolved by the ridge regression approach, the correlation may be regarded as the favoured foundation for choosing TSPs. Furthermore, a strong correlation does not always indicate stability. The association among TSPs and thermal errors is quickly disrupted due to the correlation's volatility. Consequently, it is advantageous to include a technique for assessing firmness in the association computation in order to raise the calibre of TSPs. Since testability of correlation in this research was determined by uncertainty, stability and correlation were taken into account in a thorough manner while choosing TSPs.

e) TSP Selection based on Update Regression

For thermal error models using regression methods, this work suggested update regression, an adaptive updating technique that successfully integrates new information with pre-existing models. The following is how the algorithm concept is stated:

Loss function:

$$\min(\varphi) = (\vartheta \sum_{i=1}^{n}(e_i - e_i^{'})^2 + (1\text{-}\vartheta)\sum_{i=1}^{n}(\alpha_i - \alpha_i^{'})^2) \quad (11)$$

where $\alpha = (\alpha_0 \ldots \alpha_{us})$ is new model parameter to be derived, $\vartheta = [0, 1]$ is associated weight of past model. According to this work, merely a little quantity of information and a tiny ϑ are sufficient to enable the model to be updated fast and to greatly increase its accuracy. $\vartheta = 0.1$ in this investigation. When the difference between the model coefficients created using N, $N + 1$, and $N + 2$ new information is less than 10%, it is deemed that using as little information as possible to finish the model update is feasible.

III. Spectral selective TSP Approach

Because of the effect of both interior and exterior heat points, machine tools create thermal errors through machining and manufacturing. In particular, the spindle's rapid rotation produces high heating, which make the spindle and surrounding structure to thermally expand and deform. Deformation is worse when spindle speed rises due to increased heat production. When the machine is idle during the machining process for example, through finding or tool replacement the temperature drops, which cause the spindle to withdraw and introduce additional error changes. Furthermore, variations in the operator's body temperature and the temperature of the surrounding environment might cause variations in thermal inaccuracies.

a) Selective Spectral Coding and Feature Learning

The most crucial portion of a thermal signal's distortion is determining information about specific area characteristics. They may help distinguish between those who are impacted and those who are not on a thermal map. Since deformation is a random attribute, the thermal plot thermal signal does not give any information about it. For this reason, the thermal signal is divided into several zones. The first segmentation by thresholding method was the Otsu Method [22]. Additional concern have to be taken to decide suitable standard deviation parameter values so that the method is robust enough to account for strong gradients, even though the rejection criteria ensure that the algorithm does not ignore curvilinear characteristic with smaller dissimilarity, such as surges in the observing area. [23] Recommended defining the thermal limit by means of dynamic contour models. Nevertheless, this technique discards coefficients with substantial gradients.

b) Bound Limits for TSP selection

Thresholding is used in spectral analysis to identify separate feature components. The Otsu approach, which classifies the observed spectral values as needed or distorted values based on spectral deviations, is used to calculate threshold values.

The average value of observing (N) coefficients, which is determined by averaging across all coefficients as follows, is used to apply the Otsu thresholding:

$$THo_i = \frac{So_i}{Co}, Ps_i \geq 0, \sum_{i=1}^{Co} THo_i = 1 \qquad (12)$$

Where,

$$Ps = Occ \,/\, sum(Occ) \qquad (13)$$

The two different classes (mc_0, mc_1) of observation coefficients define specific and irrelevant information.

$$\mathrm{Ks}_0 = \Pr(mc_0) = \sum_{i=1}^{k} Ps_i = \mathrm{Ks}(k) \qquad (14)$$

$$\mathrm{Ks}_1 = \Pr(mc_1) = \sum_{i=k+1}^{Co} Ps_i = 1 - \mathrm{Ks}(k) \qquad (15)$$

Where cluster mc_1 is for 1–Ks and cluster mc_o is detected by the increasing sum (ps);

Two types of coefficients are distinguished: mc_1 as objects and mc_0 as characteristics.

$$\xi(k) = \sum_{i=1}^{k} iPs_i \qquad (16)$$

Following formula is used to get the mean:

$$\xi_r = \xi(L) = \sum_{i=1}^{L} iPs_i \qquad (17)$$

To get the class discrepancy the formula used is,

$$\mu_r^2 = \sum_{i=1}^{L} (i - \xi_r)^2 Ps_i \qquad (18)$$

The selection is developed as a maximization convergence function defined as,

$$\mu_b^2(k') = \max_{l \leq k \leq L} \mu_b^2(k) \qquad (19)$$

The outcomes of thermal signal segmentation are trimmed to enhance the focus of the thermal signal object being analyzed. To cut the thermal signal, you must recognize its top, bottom, right, and left boundaries. By looping over each coefficient, these boundaries are produced; if a coefficient with an intensity of one (1) is discovered in the loop, the coefficients make up the thermal signal's boundary. Looping is done in both horizontal and vertical directions. Once boundary is identified, the thermal signal is detected for specified boundary.

The magnitude thermal signal that was gathered is used to determine the spectral density for a particular non-distorted zone. The data reveals spectral density lies in the range of 3–4 units for non-informative zone, whereas 1-2 units indicate a spectral density fluctuation with thermal error variance. The observed spectral density of a non-informative area is almost double that of the suspected regions. A suspicious region is estimated using this spectral variation. The returned area is then further processed using the directional filter-based approach to take out distortion region.
The first filter coefficient has to be specified initially since they are multiplied and added. In order to perform distortion removal and estimate the orientation field from the processed thermal plot, in 8 orientations. The

obtained thermal plot sample may show a flat scattered thermal signal with different line forms and luminous mass patches. The line orientation is extracted from the thermal plot using an orientation-based filtering technique.

c) Selective Approach of TSP

The orientation field is computed using the average thermal signal that was collected for the orientation output.

$$\alpha(i,j) = -\frac{\pi}{2} + Ps_{avg}\frac{\pi}{Ps} \qquad (20)$$

The area that varies directionally from the original region is then calculated by designing a directional filter using the average estimated orientation field.

The area of interest for the retrieved standard orientation result is taken from the 2D-directional variations that are extracted using the directional filter. The filtered input thermal signal often contains deformed and non-deformed regions in addition to smooth sections. To attain directional changes, a tree-structured filter bank consisting of eight channels is used, where the kernel is defined by,

$$\omega = \sum_{i=0}^{K-1}\left(\sum_i f_r(-i)h_i(i) - 1\right) \qquad (21)$$

Here, recursive addition and multiplication procedures are used to illustrate the convolution operation. "f" stands for the thermal signal coefficient, "h" for the filter coefficient, "I" for the process coefficient, "r" for the dimension index, and "ω" for the decimation factor. After multiplying the current filter coefficient by the previous coefficient of the thermal signal matrix, three components are finally added. The Orientational parameter for spectral variation detection is illustrated in Figure 1.

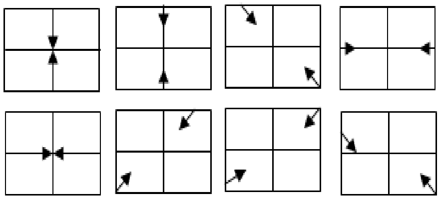

Figure 1: Orientational parameter for spectral variation recognition.

Thermal plot information must thus be treated in order to remove distortion and estimate the field from the processed thermal plot. The obtained thermal plot may show a flat variation of thermal signal with different line forms and luminous mass patches. The line orientation is extracted from the thermal plot using an orientation-based filtering technique. The spectral distribution of a thermal plot heat signal is shown in Figure 2.

.

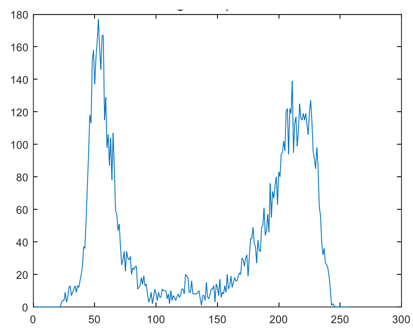

Figure 2. Energy variation in a spectrum of thermal spectral plot

The dynamic threshold used to determine the bounding area selection is provided by,

$$R_{Sel} = \begin{cases} THo_1\ ,\ if(|mc_1^2| < |mc_2^2| < |mc_3^2|), else \\ THo_2\ ,\ if(|mc_2^2| < |mc_1^2| < |mc_3^2|), else \\ THo_3 if(|mc_3^2| < |mc_1^2| < |mc_2^2|) \end{cases} \quad (22)$$

Here is an illustration of the threshold-setting procedure.
The feature coefficient is chosen using the maximal spectral energy. The following defines the threshold:

$$TSP_{th} = 0.5(\max(Ss_{Sel})) \quad (23)$$

The selection of the TSP is illustrated in Figure 3.

$$THo_f(ii) = So_{Sel}(ii, jj) \geq TSP_{th} \quad (24)$$

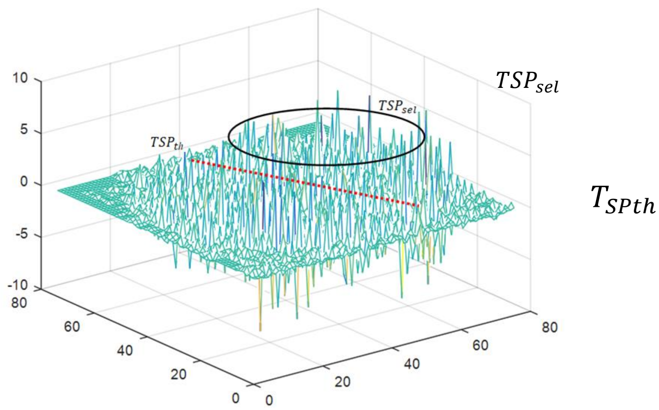

Figure 3: Selection approach of spectral coefficient in thermal error detection.

d) Feature Analysis

The bands that were selected based on their spectral characteristics are then used for classification modelling after GLCM Harrick feature extraction.
The algorithm determines which set of features to use since the optimum number of these features controls complexity and also considers optimality, reliability, and discrimination. When choosing efficient features, there will be a lot of variety. Therefore, choose the traits based on their interactions with each other. Using a co-occurrence matrix, nine feature characteristics are computed for localized area.

To quantify variance, in selected spectral region following features are computed as follows:

$$Mean(\xi) = \frac{1}{i \times j} \sum_{i=1}^{R} \sum_{j=1}^{Co} IS(i, jj) \quad (25)$$

$$\text{Vr} = \frac{1}{i \times j} \sum_{i=1}^{R} \sum_{j=1}^{Co} (IS(ii, jj) - \xi)^2 \quad (26)$$

$$\text{Std} = \sqrt{\frac{1}{i \times j} \sum_{i=1}^{R} \sum_{j=1}^{Co} (IS(ii, jj) - \xi)^2} \quad (27)$$

$$\text{Cntr} = \sum_{j=0}^{Co-1} I_i S(ii - jj)^2 \quad (28)$$

$$\text{Kurt} = \frac{1}{i \times j} \sum_{i=1}^{R} \sum_{j=1}^{Co} [(\frac{(SI(iii, j) - \xi)}{\mu})^4] - 3 \quad (29)$$

$$\text{Sm} = -\frac{1}{(1 + varianceVr^2)} \quad (30)$$

The predictions of the ELM model are developed with the extracted features and classified using CNN model.

IV. Simulation result

To assess the suggested work, thermal plot thermal signal samples are used to test the developed approach. In 19 test samples utilized to assess the proposed approach, the isolated zone is effectively identified. The location is identified when 15 more distorted heat signals are added to the test information. Of the 19 tests, the estimated properly identified area is found in 17 samples. The system sensitivity is 89%, with around 17 of the 19 classes correctly detected.

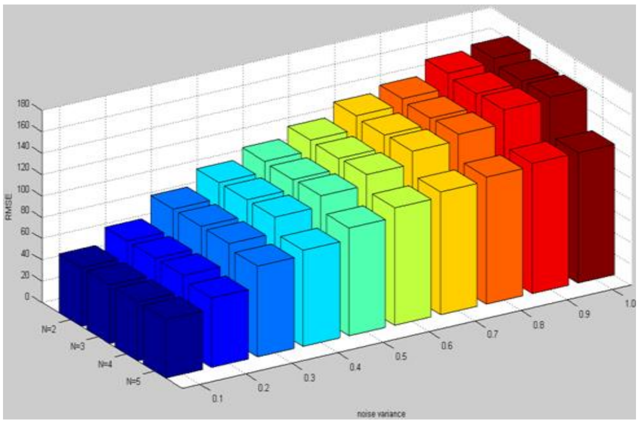

Figure 4. RMSE variation observed with varying distortion in spectral observation

Figure 4. Illustrates the change in spectral density at varying distortion level for different observing scale levels. With increase in distortion level it is observed that the higher spectral density is more effective observed. The change in spectral level is used in the detection and compensation of thermal error in machine tool operation. Table 1 shows the accuracy in identifying the area of interest for different test case with varying thermal error level.

Table 1. Accuracy (%) for error detection

Test case	Proposed (SS-ELM) model	SO-ELM model	1D-CNN model	Regression Model
S1	94.4	91.68	90.05	89.80
S2	95.1	92.67	91.35	91.78
S3	93.2	89.52	82.12	79.22

The accuracy is derived by calculating detection accuracy as a correlation between the selected area and the ground truth regions that were extracted given by,

$$Seg_{Acc} = \left(1 - \sum_{i=1}^{n} \sum_{j=1}^{mc} \left|Rg_{i,j} - RSo_{i,j}\right|\right) \times 100 \qquad (31)$$

where Rg is the ground truth thermal signal and Rs is the system-processed segmented thermal signal for m×n dimension. The proposed technique offers a 3-4% increase in accuracy compared to existing methods. The created technique's observations are shown in the observations that follow. The mean square error (MSE) observation for the developed system is shown in Figure 5. Examination demonstrates that change in distortion level defined by the variance level is controlled by the proposed spectral selective-ELM (SS-ELM) as compared to exiting methods. The finer selection approach by the proposed method obtains a higher error detection resulting into more tolerance and compensation means to thermal error detection.

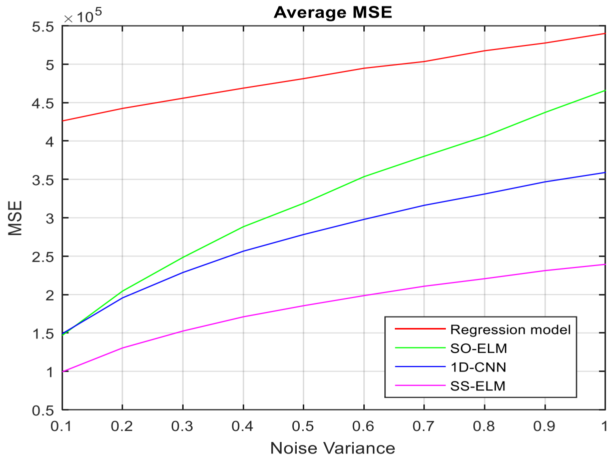

Figure 5. Mean error observation by different learning methods

Table 2: Observation for MSE in thermal error detection

variance	Methods			
	Regression model	SO-ELM	1D-CNN	SS-ELM
0.1	0.29	0.13	0.12	0.1
0.3	0.57	0.15	0.15	0.04
0.5	1.14	0.30	0.16	0.06
0.6	1.87	0.51	0.21	0.12
0.7	2.74	1.33	0.45	0.21
0.9	3.85	2.41	1.44	0.52

The peak signal to noise ratio (PSNR) is measured as observation of measure error with reference to observed spectral signals. The PSNR defines the accuracy of spectral feature selection and a higher PSNR detection reflects a greater accuracy in accurate signal detection. Observation shown in Figure 6. Illustrates the significance of proposed SS-ELM method in detection of spectral feature resulting in accurate thermal error.

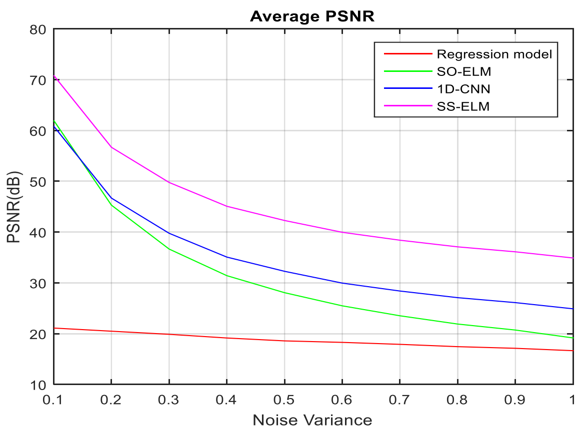

Figure 6: Peak SNR for developed method in thermal error detection

Table 3: observation of PSNR (dB) for different learning approaches

variance	Methods			
	Regression model	SO-ELM	1D-CNN	SS-ELM
0.1	38	73	75	76
0.3	25	42	85	83
0.5	14	45	53	74
0.6	17	28	42	56
0.7	18	22	32	48
0.9	14	21	21	35

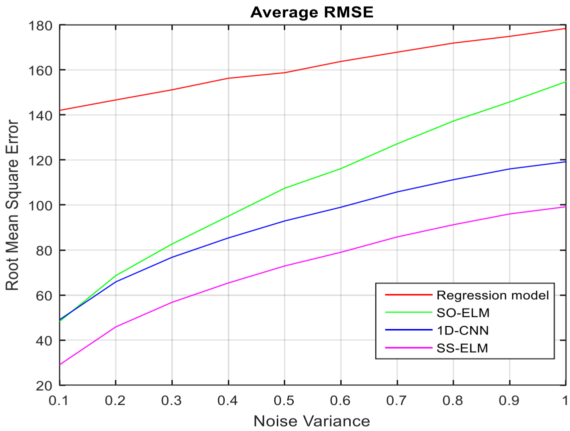

Figure 7: RMSE for the developed learning methods for thermal error detection

Table 4: observation for RMSE parameter

variance	Methods			
	Regression model	SO-ELM	1D-CNN	SS-ELM
0.1	34	11	6	2
0.3	72	22	15	5
0.5	71	41	19	7
0.6	122	71	25	11
0.7	134	111	57	32
0.9	155	152	113	53

The RMSE of the proposed SS-ELM technique, which is determined by taking the squared root of the MSE parameter, is 2.72% lower than that of the 1D-CNN and 3.51% lower than that of the SO-ELM at noise variance σ = 0.6. When the RMSE is 0, the method correctly identifies each spectral variation and gets the relevant information for the processing error. The relative reconstruction error (RRE) observation with varying noise variance is shown in Figure 8.

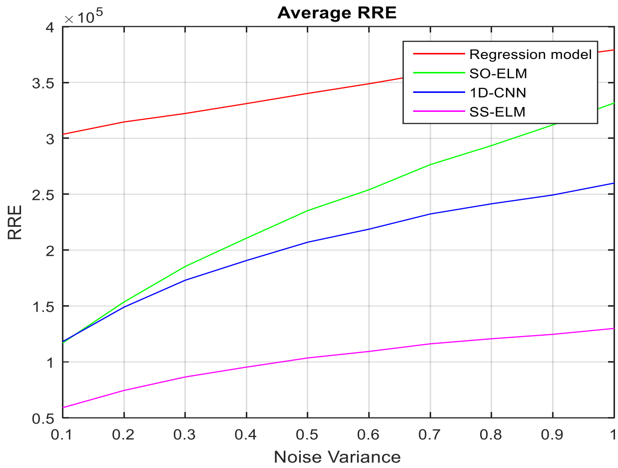

Figure 8: RRE plot for developed learning approach in thermal error detection

Table 5: observation for RRE for developed approaches

variance	Methods			
	Regression model	**SO-ELM**	**1D-CNN**	**SS-ELM**
0.1	2.33	0.34	0.14	0.13
0.3	3.84	0.41	0.16	0.11
0.5	4.83	0.86	0.5	0.14
0.6	5.54	1.5	0.4	0.23
0.7	5.86	1.2	0.6	0.5
0.9	7.01	2.6	0.76	0.2

It is observed that the proposed SS-ELM approach has a lower relative reconstruction error as it employs a dynamic decision for the spectral detection. The method shows a lower relative reconstruction error as the measurement level was generated using threshold rules. Furthermore, the estimated features can withstand high distortion in spectral densities. This demonstrates the accuracy of the proposed technique in thermal error detection.

V. conclusion

One of the key elements influencing machine tool machining precision is thermal error. A model developed on one device may be transferred to another using transfer learning in thermal error Modelling. For accurate region estimate, the developed system shows how the proposed approach needs less complexity. The directional filter estimate approach based on the determined orientation field reduces the number of estimation iterations by estimating the orientation field across a given direction. The developed system has a better estimate accuracy because of its increased overall system sensitivity. Technique for predicting supporting features demonstrates how to develop an automated system for categorizing thermal plot impacts so that they may be automatically identified. The proposed approach combines the transformation technique with orientation filtering. The work indicates that the orientation approach's use the method providing more detailed information that helps resolve finer distortion. The approach provided a simple and effective means of automation in thermal error detection.

VI. Reference

[1] L. Peng, Z.L. Chen, L.L. Cheng, et al., Research on optimal multivariate thermal error Modelling based on finite-element analysis, Proc. IME E J. Process Mech.Eng. (2023) Mar, 2023.

[2] Y. Li, Q.A. Chen, F. Gao, et al., Synthetic positioning error Modelling for a linear feed system based on GA-SVR algorithm, J. Braz. Soc. Mech. Sci. Eng. 45 (2)(2023) Feb.

[3] Q. Yin, F. Tan, H.X. Chen, et al., Spindle thermal error Modelling based on selective ensemble BP neural networks, Int. J. Adv. Manuf. Technol. 101 (5–8) (2019)1699–1713 APR.

[4] G.Q. Fu, C. Tao, Y.P. Xie, et al., Temperature-sensitive point selection for thermal error Modelling of machine tool spindle by considering heat source regions, Int.J. Adv. Manuf. Technol. 112 (9–10) (2021) 2447–2460 FEB.

[5] C.C. Chen, H.J. Dai, C. Lee, et al., The development of thermal error compensation on CNC machine tools by combining ridge parameter selection and backwardelimination procedure, Int. J. Adv. Manuf. Technol. 16 (2023 DEC) 2023.

[6] M. Zhu, Y. Yang, X. Feng, et al., Robust Modelling method for thermal error of CNC machine tools based on random forest algorithm, J. Intell. Manuf. 34 (4)(2023) 2013–2026 2023/04/01.

[7] H. Ye, X. Wei, X. Zhuang, et al., An improved robust thermal error prediction approach for CNC machine tools, Machines 10 (8) (2022) 624.

[8] H. Liu, E.M. Miao, X.Y. Wei, et al., Robust Modelling method for thermal error of CNC machine tools based on ridge regression algorithm, Int. J. Mach. ToolManufact. 113 (2017) 35–48 2017/02/01/.

[9] Q.Y. Teng, Z. Liu, Y.Q. Song, et al., A survey on the interpretability of deep learning in medical deformation, Multimed. Syst. 28 (6) (2022) 2335–2355 DEC.

[10] J.W. Xing, T. Nagata, X.Y. Zou, et al., Achieving efficient interpretability of reinforcement learning via policy distillation and selective input gradient regularization, Neural Network. 161 (2023) 228–241 APR.

[11] G.Q. Fu, H.W. Gong, H.L. Gao, et al., Integrated thermal error Modeling of machine tool spindle using a chicken swarm optimization algorithm-based radial basicfunction neural network, Int. J. Adv. Manuf. Technol. 105 (5–6) (2019) 2039–2055 DEC.

[12] X.S. Gao, K. Zhang, Z.T. Zhang, et al., XGBoost-Based Thermal Error Prediction and Compensation of Ball Screws, Proceedings Of The Institution Ofmechanical Engineers Part B-Journal Of Engineering Manufacture, 2023 2023 Feb 27.

[13] B.L. Jian, C.C. Wang, C.T. Hsieh, et al., Predicting spindle displacement caused by heat using the general regression neural network, Int. J. Adv. Manuf. Technol.104 (9–12) (2019) 4665–4674 OCT.

[14] B.L. Jian, C.C. Wang, H.T. Yau, et al., Optimization of lathe cutting parameters using taguchi method and grey relational analysis, Sensor. Mater. 32 (3) (2020)843–858.

[15] X. Wei, H. Ye, E. Miao, et al., Thermal error Modelling and compensation based on Gaussian process regression for CNC machine tools, Precis. Eng. 77 (2022)65–76.

[16] H. Liu, H. Motoda, Feature transformation and dimensionality reduction, in: H. Liu, H. Motoda (Eds.), Feature Selection for Knowledge Discovery and InformationMining, Springer US, Boston, MA, 1998, pp. 151–187.

[17] R.O. Duda, P.E. Hart, D.G. Stork, Pattern Classification, second ed., Wiley-Interscience, 2000.

[18] D.C. Montgomery, Design and Analysis of Experiments, John Wiley & Sons, Incorporated, 2017.

[19] J.V. Deshpande, U. Naik-Nimbalkar, I. Dewan, Nonparametric Statistics: Theory and Methods, World Scientific, 2018.

[20] Z.E. Aydin, Z.K. Ozturk, Filter-based feature selection methods in the presence of missing information for medical prediction models, Multimed. Tool. Appl. 83 (2023)24187–24216 Aug, 2023.

[21] Li, Z.; Li, G.; Xu, K.; Wang, L.; Zhang,W. Thermal Error Analytical Modelling of Gear Grinding Machine Full-Closed-Loop FeedSystem Based on Equivalent Temperature Field. Mech. Syst. Signal Process. 2025, 224, 112105.

[22] Liu, Xueli, Zhanlong Zhang, Yuefeng Hao, Hui Zhao, and Yu Yang. "Optimized OTSU segmentation algorithm-based temperature feature extraction method for infrared images of electrical equipment." *Sensors* 24, no. 4 (2024): 1126.

[23] Yang, Hong, and Jun Ni. "Dynamic modeling for machine tool thermal error compensation." *J. Manuf. Sci. Eng.* 125, no. 2 (2003): 245-254